A&A 436, 977–982 (2005)
DOI: 10.1051/0004-6361:20052764

Astronomy & Astrophysics

Upper limits on CO 4.7 μm emission from disks around five Herbig Ae/Be stars⋆

A. Carmona[1,3], M. E. van den Ancker[1], W.-F. Thi[2], M. Goto[3], and Th. Henning[3]

[1] European Southern Observatory, Karl Schwarzschild Strasse 2 , 75748 Garching bei München, Germany
e-mail: acarmona@eso.org
[2] Astronomical Institute, University of Amsterdam, Kruislaan 403, 1098 SJ Amsterdam, The Netherlands
[3] Max Planck Institute for Astronomy, Königstuhl 17, 69117 Heidelberg, Germany

Received 25 January 2005 / Accepted 14 March 2005

Abstract. We present the results of medium-resolution spectroscopy of five nearby Herbig Ae/Be stars at 4.7 μm: UX Ori, HD 34282, HD 50138, V380 Ori, HK Ori. The goal was to search for CO fundamental ro-vibrational emission. None of the targets show CO features, either in absorption nor in emission. We derive a 5σ upper limit of $<10^{-12}$ cm^{-2} to the column density of hot CO ($T \approx 1500$ K) in the sources. These upper limits are considerably lower than the values of Herbig Ae/Be stars for which warm and hot CO emission has been reported. The non-detection of CO $\nu = 1-0$ emission in these five targets suggest that Herbig Ae/Be stars are not a homogeneous group with respect to the structure of the gaseous disk and/or the amount of CO in the inner 50 AU of their disks.

Key words. stars: circumstellar matter – stars: planetary systems: protoplanetary disks – stars: planetary systems: formation – stars: pre-main sequence

1. Introduction

Circumstellar disks around pre-main sequence stars are the likely place for planet formation. Present theoretical models predict that planets are formed in the inner 50 AU of such disks. Terrestrial planets are thought to be made from hierarchical grouth of planetesimals (e.g. Ida & Lin 2004). Two major classes of models exist for the formation of gas giant planets: a) the gravitational instabilities model (Boss 2004; Mayer et al. 2004), b) the core accretion model (Pollack 1996; Alibert et al. 2004; Kornet et al. 2002). The knowledge of fundamental disk properties such as temperature and density profile, geometry and dissipation time scales, gas and dust composition, is paramount to constrain planet formation models.

Giant planets in our Solar System and giant extrasolar planets (Vidal-Madjar et al. 2004) are composed mainly of gas. Current models predict that they are formed in the inner 50 AU of the protoplanetary disk (Ida & Lin 2004; Alibert et al. 2004; Boss 2004). However, the observational study of the gas in the planet forming region of the disks only started recently with the advent of space observatories (e.g. Bergin et al. 2004; Thi et al. 2001; Lecavellier des Etangs et al. 2003) and high-resolution infrared spectrometers mounted on large aperture telescopes (e.g. Richter et al. 2002; Bary et al. 2002, 2003; Brittain & Rettig 2002; Brittain et al. 2003; Najita et al. 2000, 2003; Blake & Boogert 2004).

Intermediate-mass Herbig Ae/Be stars (HAEBES) and low-mass classical T Tauri stars are pre-main sequence stars characterized by strong optical emission lines (e.g. Hα) and infrared excess. These properties are consistent with the idea that they are young stars surrounded by a circumstellar disk. The strong emission lines are interpreted as the signature of gas accretion onto the central star, and the infrared excess as the emission of the warm dust in the disk (see reviews by Waters & Waelkens 1998 and Bertout 1989). These disks have been imaged from the NIR to the (sub-)millimetre (e.g. Grady et al. 2004; Mannings & Sargent 1997, 2000; Henning et al. 1998). Nearby HAEBES and T Tauri stars are natural laboratories for studying the process of planet formation.

Pure rotational CO emission from circumstellar disks is commonly seen at millimeter and submillimeter wavelengths (e.g. Qi et al. 2004; Ceccarelli et al. 2002; Mannings & Sargent 2000; Thi et al. 2004). However, these wavelengths are only sensitive to the cold gas ($T < 50$ K) in outer regions of the disk ($R > 50$ AU).

Theoretical models and recent observational evidence suggest that in the inner 50 AU, temperatures can be relatively high ($T \geq 150$ K) (Willacy et al. 1998; Dullemond et al. 2001; Markwick et al. 2002; Kamp & Dullemond 2004). Under these conditions, molecules such as water and CO are in the gas phase, and a rich emission spectrum from their rotational and vibrational transitions is expected. However, the relatively large column densities in the inner 50 AU (1500 g cm^{-2} at 1 AU for the minimum-mass solar nebula) could preclude the

⋆ Based on observations collected at the European Southern Observatory, Chile (program ID 072.C-0535).

observability of such transitions, because the disk is optically thick in the continuum (Najita et al. 2003).

Nevertheless, in some circumstances, parts of the inner circumstellar disk could be optically thin, and warm CO emission becomes detectable. Carr et al. (2001), Brittain & Rettig (2002) and Rettig et al. (2004) detected $\nu = 1-0$ emission of warm CO and suggested that it originates in a disk gap or in a inner low-density region; Najita et al. (2000, 2003) and Blake & Boogert (2004) reported the detection of CO fundamental ro-vibrational band, and postulated that warm CO emission is produced in a disk's atmosphere when the stellar radiation of the host star induces a temperature inversion (disk atmosphere hotter than the disk mid-plane); Brittain et al. (2003) found $\nu = 1-0$ emission of hot and warm CO in AB Aur and suggested that it is produced by IR pumping (resonant scattering). The same authors reported the detection of $\nu = 2-1$ and $3-2$ emission of CO in HD 141569, and pointed out that it originates by UV pumping in the inner rim of the disk.

This paper describes our search for CO fundamental ro-vibrational emission from a selected number of Herbig Ae stars known to be surrounded by a disk. Meeus et al. (2001) devised a classification scheme for the spectral energy distributions (SED) of Herbig Ae/Be stars. In their classification scheme, group I sources have a SED that is strongly double-peaked in the near to mid-infrared, whereas the SED of group II sources can be described by a power-law at those wavelengths. Dullemond (2002) has identified this empirical classification with two different disk geometries: flared (group I) and self-shadowed (group II). We observed objects belonging to both groups. UX Ori, V380 Ori, HK Ori (group I) are likely to have a flared disk, and HD 50138 and HD 34282 (group II) a self-shadowed disk. We used ISAAC at the VLT at $R \sim 10\,000$ to search for the CO emission band at 4.7 μm. We report here our non detection in all the objects observed in April 2004. We discuss how the stringent upper limits derived from our deep search set constrains the physical properties of the observed disks.

The paper is organized as follows. In Sect. 2 the observational set-up and data reduction procedure are described, in Sect. 3 the spectra obtained and the estimation of the upper limits to the hot ($T \approx 1500$ K) CO column density are presented, finally in Sect. 4 the meaning of our results in the context of the structure of the disk is discussed.

2. Observations

Medium-resolution spectra in the 4.6–4.8 μm range were obtained for five Herbig Ae/Be stars (UX Ori, HD 34282, HD 50138, V380 Ori and HK Ori) between the 2nd and 20th of April 2004 using ISAAC at the First Unit Telescope ANTU of the ESO-VLT at Cerro Paranal, Chile. These targets were selected to maximize the shift in velocity between the expected position of the CO emission in the targets and the telluric CO absorption at the time of observation. A medium-resolution grating and the narrowest available slit (0.3″) were used to provide spectra of resolution 10 000. The slit has been oriented in the North-South direction. Sky background was subtracted by chopping each exposure by 15″ in the direction of the slit. Asymmetrical thermal background of the telescope was subtracted by nodding the telescope by 15″. In each nodding position the telescope has been randomly jittered in order to record the raw spectra in different regions of the detector, minimizing the influence of bad pixels. In order to correct telluric absorption and obtain absolute flux calibration, spectroscopic standard stars were observed the same night at airmasses close to that of the science targets. Dome flat fields were obtained at the beginning and at the end of each observing night.

2.1. Data reduction

Chopped raw frames of each nodding position were first corrected for the detector non-linearity. Since half-cycle frames were not recorded, the median value of each frame was subtracted to obtain an approximation to the half-cycle frame intensity subject to non-linearity. The residual raw frame was corrected for non-linearity using the expression

$$F_{\rm c} = f_{\rm rr} + 1.05 \times 10^{-6} \times f_{\rm rr}^2 + 0.85 \times 10^{-10} \times f_{\rm rr}^3$$

in which $F_{\rm c}$ refers at the corrected frame, and $f_{\rm rr}$ is the residual raw frame[1]. Once this correction for detector non-linearity is made, the median previously subtracted is added back to the frame.

The second step in the data reduction procedure is to correct all the frames for tilt in the spatial direction using Ar Xe arc lamp frames taken the same day of the observations. A second order polynomial deduced from the arc file is used for this correction. Individual exposures are corrected for differences in the detector sensitivity by dividing them by normalized dome flat fields.

Flat-fielded frames were combined using the Eclipse[2] jittering procedure. The procedure consists in classifying the set of data in groups having the nodding sequence form ABBA. In each group, the frames in the A position and B position are averaged, the averaged frames are subtracted from each other, divided by 2, and a combined frame is generated ($F_{\rm combined} = (\bar{A} - \bar{B})/2$). The ensemble of combined frames, one for each ABBA group, are stacked in one single final 2D frame. During this process, combined frames are shifted in such a way that the addition of all the spectra is located in the center of the the final frame. This shifting procedure optimizes the subtraction of sky and telescope background emission.

One-dimensional spectra are extracted from the 2D frame, averaging the pixel counts in the PSF direction. These spectra are then divided by the exposure time defined by

$$E_{\rm time}[{\rm s}] = {\rm DIT} \times {\rm NDIT} \times 2 \times {\rm Chopcycles}.$$

Here DIT is the Detector Integration Time (1.84 s in our case), NDIT is the number of DIT and Chopcycles is the number of chopping cycles (8) per DIT.

[1] Values taken from the ISAAC data reduction manual, see www.eso.org/instruments/isaac/#Documentation

[2] www.eso.org/eclipse

Table 1. H I lines detected in the 4.6–4.8 μm spectra of our targets.

		UX Ori	HD 34282[a]	HD 50138	V380 Ori	HK Ori
Line		Pf β	–	Pf β	Pf β	Pf β
Central Wavelength (λ)	[μm]	4.655	–	4.656	4.655	4.655
FWHM	[km s^{-1}]	255	–	156	176	233
Equivalent Width (*EW*)	[Å]	−7.4	–	−11.7	−12.7	−5.1
Line Flux (F_λ)	[W m^{-2}]	2.3×10^{-16}	–	5.1×10^{-15}	1.5×10^{-15}	1.1×10^{-16}
Line		Hu ε	–	Hu ε	Hu ε	–
Central Wavelength (λ)	[μm]	4.674	–	4.675	4.673	–
FWHM	[km s^{-1}]	60	–	142	116	–
Equivalent Width (*EW*)	[Å]	−3.2	–	−6.7	−4.1	–
Line Flux (F_λ)	[W m^{-2}]	1.0×10^{-16}	–	3.0×10^{-15}	4.7×10^{-16}	–

[a] No H I lines were detected in the ISAAC spectra of HD 34282.

The one-dimensional spectrum of the standard star is corrected for the differences in airmass and air pressure with the science target using,

$$I_{\mathrm{STD}_{\mathrm{corrected}}} = I_0 \ \exp\left(-\tau \ \frac{\bar{X}_{\mathrm{TARGET}}}{\bar{X}_{\mathrm{STD}}} \ \frac{\bar{P}_{\mathrm{TARGET}}}{\bar{P}_{\mathrm{STD}}}\right).$$

Here $\bar{X}$ is the average of the airmass and $\bar{P}$ is the average of the air pressure. The continuum I_0 has been defined as uniform with a value equal to the mean plus three standard deviations ($I_0 = \bar{I}_{\mathrm{obs}} + 3\sigma_{I_{\mathrm{obs}}}$). The optical depth τ has been calculated from the measured data using $\tau = \ln(I_{\mathrm{obs}}/I_0)$.

Employing a synthetic model of the earth atmosphere, the extracted one-dimensional spectra of the target and the standard star were subject to a precise wavelength calibration involving a correction for differences in the spectral resolution of both stars (Goto et al. 2003).

Finally, the science target spectrum is flux calibrated and corrected for atmospheric absorption by dividing it by the corrected spectrum of the standard star. Absolute flux calibration is obtained by multiplying the telluric corrected spectra by a theoretical SED model (Kurucz 1991) of the standard star.

We estimate the uncertainty in the flux calibration of our spectra to be between 10% and 20%. The principal source of noise in the spectra is due to imperfections in the correction for telluric absorption. The 4.7 μm band is particularly challenging in this aspect given the presence of strong CO absorption in the earth's atmosphere. Although the standard stars were observed with airmasses close to those of the science targets, and the extracted spectra were corrected for differences in airmass, air pressure and spectral resolution, in the regions of poor atmospheric transition the correction for the telluric absorption is not perfect. The noise present in the spectra is mostly due to systematic errors in this correction.

3. Results

Flux calibrated spectra of the five Herbig Ae/Be stars are presented in Fig. 1. The $v = 1{-}0$ ro-vibrational band of CO was not detected in any of our targets, neither in absorption nor in emission. The only notable feature in all the spectra (except HD 34282) are recombination lines of H I: Pf β, Hu ε. A summary of the H I observations is presented in Table 1. In the case of HD 293782 and HK Ori the Pf β line shows a strong red/blue asymmetry. This phenomenon is likely associated with infalling gas (Najita et al. 1996). HD 50138 and V380 Ori show symmetric Pf β profiles. In these two systems the Hu ε emission line has a strong blue/red asymmetry and extended blue wings. This line most likely originates in a similar region as the balmer lines of H I, which are believed to come from a wind either from the disk or the central star (see Bouret & Catala 1998, 2000).

We derived upper limits to the flux in the CO emission line taking a conservative 5σ (standard deviation) of the intensity in the continuum ($\sigma_{I_{\mathrm{obs}}}$). Given that the minimum *FWHM* of the instrument is 4.7×10^{-4} μm, we obtained upper limits ranging from 2.2×10^{-17} to 5.9×10^{-17} W m^{-2} for UX Ori, HD 34282, HK Ori, V380 Ori, and 4.2×10^{-16} W m^{-2} for HD 50138 (see Table 2).

From the upper limit to the CO flux, and supposing that CO is excited by infrared fluorescence (resonant scattering), we estimated the upper limit to the column density of hot CO using Brittain et al. (2003)[3]:

$$N = \frac{4\pi F_{\mathrm{line}}}{\Omega \ g_{\mathrm{line}} \ h\, c\, \tilde{\nu}}.$$

Here F_{line} is the $v = 1{-}0$ line flux, Ω is the solid angle, $h\, c\, \tilde{\nu}$ is the energy per photon, and $g_{\mathrm{line}} = P_J\, g_{1-0}$ is the fluorescence efficiency for the 1−0 ro-vibrational transition by IR pumping.

[3] Originally in DiSanti et al. (2001).

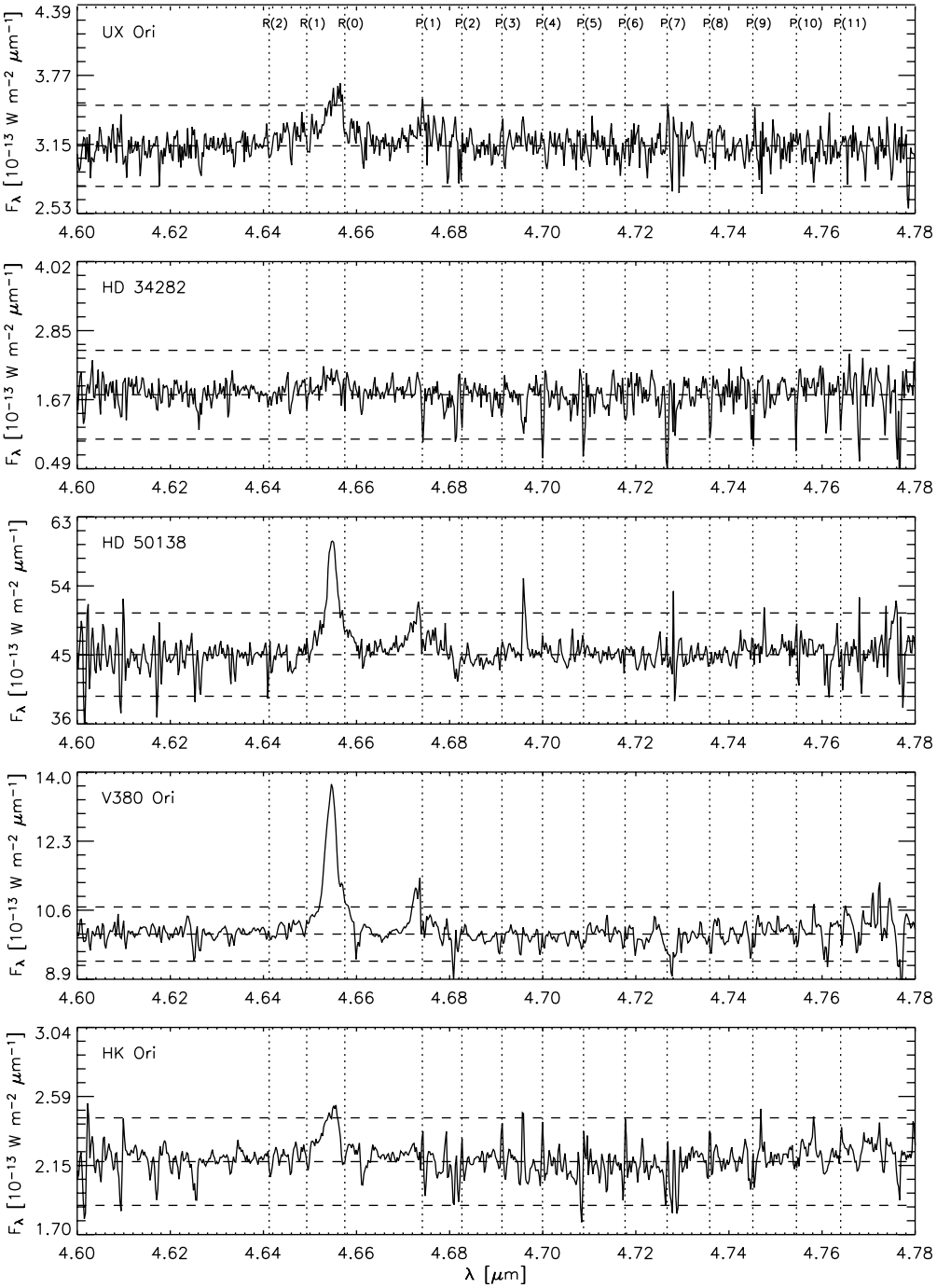

Fig. 1. ISAAC spectra of our five target stars. The strong emission seen at 4.65 μm and 4.67 μm are the Pf β and Hu ε recombination lines of H I. The noise in the spectra is mostly due to systematic errors in the telluric correction in this region of poor atmospheric transmission. Vertical dotted lines show the CO $v = 1-0$ transitions. Horizontal dashed lines show the 3σ limits of the intensity.

Brittain et al. (2003) estimated a g_{1-0} at 0.6 AU of 1.1 photons molecule^{-1} s^{-1} for AB Aur, and calculated a column density of observed hot CO of 2×10^{13} cm^{-2}. Given that UV pumped ($v = 2-1$) transitions were not detected in the wavelength range observed (4.6–4.8 μm), and assuming that our observed HAEBES have an inner disk configuration similar to AB Aur, we scaled the g_{1-0} coefficient for each star based on the IR luminosity ($L_{\mathrm{IR}_\star}$) at 4.7 μm and the distance ($d_\star$) employing[4]

$$g_{1-0\,\star} = g_{1-0_{\mathrm{AB\,Aur}}} \frac{d_\star^2 \times L_{\mathrm{IR}_\star}}{d_{\mathrm{AB\,Aur}}^2 \times L_{\mathrm{IR}_{\mathrm{AB\,Aur}}}}.$$

With this estimate of g_{1-0} for each of our targets and the upper limit for the line flux we calculated the hot CO column density.

[4] AB Aur is a 144 pc and has a 4.7 μm intensity of 1.47×10^{-12} W m^{-2} μm^{-1}.

Table 2. Summary of CO $\nu = 1$–0 emission characteristics of our sample stars.

		UX Ori	HD 34282	HD 50138	V380 Ori	HK Ori	AB Aur[a]
Distance[b]	pc	400	164	290	500	500	144
Average Intensity	[10^{-13} W m^{-2} μm^{-1}]	3.1	1.8	44.7	10.0	2.2	14.7
5σ	[10^{-13} W m^{-2} μm^{-1}]	0.6	1.3	9.0	1.1	0.5	–
S/N		25	7	25	45	23	–
Instrument *FWHM*	[10^{-4} μm]	4.7	4.7	4.7	4.7	4.7	–
Line Flux upper-limit	[10^{-17} W m^{-2}]	<2.9	<5.9	<42	<5.2	<2.2	8.6
scaled g_{1-0}	pho mol^{-1} s^{-1}	1.8	0.2	13.6	9.0	2.0	1.1
Column density of hot CO (1500 K)	[10^{12} cm^{-2}]	<4.1	<89	<8.0	<1.5	<2.9	20

[a] Values for AB Aur are listed for reference (Brittain et al. 2003).
[b] For HD 34282, HD 50138 and AB Aur the distance is estimated using Hipparcos data. UX Ori, V380 Ori and HK Ori have been assumed to be associated with the Orion OB1a (UX Ori) and OB1c (V380 Ori, HK Ori) star-forming regions.

Our results are summarized in Table 2. We find upper limits to the column density of hot CO ranging from 1.5×10^{12} to 8.0×10^{12} cm^{-2}. In the case of HD 34282 the upper limit calculated is 8.9×10^{13} cm^{-2}. However, this is not a representative limit since the signal to noise of the spectra is low ($S/N = 7$).

4. Discussion

Najita et al. (2003), Brittain et al. (2003), Blake & Boogert et al. (2004), and Rettig et al. (2004) showed how the study of warm and hot CO emission could be used as a powerful tool for probing disk surfaces and for assessing the density and temperature profiles of the inner 50 AU of the circumstellar disk independent of SED models. These authors reported the detection of the $\nu = 1$–0 transition of CO in several Herbig Ae/Be stars.

Our estimates of the upper limit to the CO line fluxes are within the range of the detections of CO $\nu = 1$–0 emission fluxes measured. For example in AB Aur Brittain et al. (2003) observed a CO $R(1)$ line flux of 8.6×10^{-17} W m^{-2} in AB Aur and Blake & Boogert (2004) detected a CO $P(2)$ line flux of 10.4×10^{-17} W m^{-2} in the same star. The upper limits to the hot CO column density calculated (except for HD 34282 that presented a low *S/N* spectrum) are well below the 2×10^{13} cm^{-2} value reported for AB Aur by Brittain et al. (2003). From the upper limits deduced from our observations, we conclude that if our targets would had equal column densities of hot CO, or had presented CO $\nu = 1$–0 emission fluxes of the magnitude reported in the literature, we would have detected this emission within our ISAAC data.

Previous studies suggested that CO emission is produced by UV pumping or by IR fluorescence (resonant scattering). The nature of the excitation mechanism is revealed from the CO transitions present in the spectra. The $\nu = 2$–1 and 3–2 emission bands indicate that the principal source of excitation is UV pumping. On the other hand, the $\nu = 0$–1 band indicates that the excitation mechanism is thermal (i.e. IR resonant scattering). Our upper limits are small enough that they are in the detection range of the $\nu = 2$–1 and 3–2 emission band previously reported in the Herbig star HD 141569 by Brittain et al. (2003), $F_{3-2} = 1.1 \times 10^{-17}$ W m^{-2}. The non-detection of UV excited CO transitions within our data suggests that UV radiation is scattered by the dust in the disk's inner rim and that the CO is probably shielded. However, the inner part of the disk ($R < 50$ AU) could also be optically thick in the continuum, precluding the observability of such transitions.

Meeus et al. (2001) in their study of the spectral energy distribution (SED) of a large sample of Herbig Ae/Be stars suggested that they could be classified in two groups according to the SED shape. Detailed modeling of the dust emission by Dullemond (2002) found that the 3 μm bump observed in many SEDs could be interpreted as evidence for the existence of a dusty "puffed-up" inner disk rim, and that the Meeus et al. classification could be understood as corresponding to two inner disk geometries: flared disk, and self-shadowed disk.

Using this geometrical classification, Brittain et al. (2003) interpreted the two temperature CO $\nu = 1$–0 profiles deduced from the rotational diagrams of AB Aur in the following way. They suggested that the hot (1500 K) CO originates just beyond the "puffed-up" inner rim by IR resonant scattering at 0.6 AU, and that the cold CO (70 K) is emitted by IR fluorescence in the surface of the flared disk at 8 AU.

Following this classification method, our targets fall in both groups of disks: UX Ori, V380 Ori, HK Ori are likely to have a flared disk, and HD 50138 and HD 34282 a self-shadowed disk. Their SEDs indicate that all of them should have a "puffed-up" inner rim. The non-detection of $\nu = 1$–0 emission in our targets suggests that there is no strong correlation between the disk geometry and CO emission properties.

Recent work by Rettig et al. (2004), shows the detection of optically thin warm ($T \approx 140$ K) CO emission in the classical T Tauri star TW Hydrae. These authors ascribed the non detection of hot CO ($T > 1000$ K) as evidence for a cleared inner disk region out to a radial distance of ≈0.5 AU, and proposed that the warm CO emission is produced in a dissipating gaseous disk. In view of this interpretation, we could conclude that the non-detection of hot CO in our targets is consistent with the idea that our stars cleared of gas in their inner gaseous disks. However, the presence of strong emission lines in the optical spectra of HAEBES testifies to the occurrence of accretion. Both results could be compatible under a scenario where

accretion and clearing are episodic and that a replenishment mechanism is active.

In summary, the non-detection of CO $v = 1-0$ emission in these five targets suggests that, *despite the relative similarity of the dust emission in Herbig Ae/Be stars, they are not a homogeneous group with respect to gas emission, and in particular to hot and warm CO emission*. This heterogeneity could be interpreted as the result of (1) differences in the structure of their inner gaseous disk leading to differences in the inner disk CO temperature; or (2) true differences in the amount of warm CO, either due to chemical effects (selective CO depletion implying a variable CO/H_2 ratio in the disk) or due to variations in the amount of bulk gas in the inner 50 AU (assuming a constant CO/H_2 ratio). The last scenario is particularly intriguing. True variations in the the bulk of H_2 in the inner disk are consistent with the idea that in these stars giant planets have already formed. Unfortunately, the present data do not allow us to confirm such a tantalizing hypothesis. Future instruments with improved spectral resolution like CRIRES at the VLT will help us to address such ideas quantitatively.

Acknowledgements. We would like to thank C.P. Dullemond and A. Bik for several fruitful discussions. The authors wish to thank the ESO-VLT staff at Paranal observatory and in Garching that performed the service-mode observations presented in this paper. This research has made use of the SIMBAD database, operated at CDS, Strasbourg, France.

References

Aikawa, Y., van Zadelhoff, G. J., van Dishoeck, E. F., & Herbst, E. 2002, A&A, 386, 622
Alibert, Y., Mordasini, C., & Benz, W. 2004, A&A, 417, L25
Bary, J. S., Weintraub, D. A., & Kastner, J. H. 2002, ApJ, 576, L73
Bary, J. S., Weintraub, D. A., & Kastner, J. H. 2003, ApJ, 586, 1136
Bergin, E., Calvet, N., Sitko, M. L., et al. 2004, ApJ, 614, L133
Bertout, C. 1989, ARA&A, 27, 351
Blake, G. A., & Boogert, A. C. A. 2004, ApJ, 606, L73
Bouret, J.-C., & Catala, C. 1998, A&A, 340, 163
Bouret, J.-C., & Catala, C. 2000, A&A, 359, 1011
Boss, A. P. 2004, ApJ, 610, 456
Brittain, S. D., & Rettig, T. W. 2002, Nature, 418, 57
Brittain, S. D., Rettig, T. W., Simon, T., et al. 2003, ApJ, 588, 535
Carr, J. S., Mathieu, R. D., & Najita, J. R. 2001, ApJ, 551, 454
Ceccarelli, C., Boogert, A. C. A., Tielens, A. G. G. M., et al. 2002, A&A, 395, 863
DiSanti, M. A., Mumma, M. J., Russo, N. D., & Magee-Sauer, K. 2001, Icarus, 153, 361
Dullemond, C. P., Dominik, C., & Natta, A. 2001, ApJ, 560, 957
Dullemond, C. P. 2002, A&A, 395, 853
Goto, M., Usuda, T., Takato, N., et al. 2003, ApJ, 598, 1038
Grady, C. A., Woodgate, B., Torres, C. A. O., et al. 2004, ApJ, 608, 809
Habart, E., Natta, A., & Krügel, E. 2004, A&A, 427, 179
Henning, T., Burkert, A., Launhardt, R., Leinert, C., & Stecklum, B. 1998, A&A, 336, 565
Ida, S., & Lin, D. N. C. 2004, ApJ, 616, 567
Jonkheid, B., Faas, F. G. A., van Zadelhoff, G.-J., & van Dishoeck, E. F. 2004, A&A, 428, 511
Kamp, I., & Dullemond, C. P. 2004, ApJ, 615, 991
Kornet, K., Bodenheimer, P., & Różyczka, M. 2002, A&A, 396, 977
Kurucz, R. L. 1991, BAAS, 23, 1047
Lecavelier des Etangs, A., Deleuil, M., Vidal-Madjar, A., et al. 2003, A&A, 407, 935
Mannings, V., & Sargent, A. I. 1997, ApJ, 490, 792
Mannings, V., & Sargent, A. I. 2000, ApJ, 529, 391
Markwick, A. J., Ilgner, M., Millar, T. J., & Henning, T. 2002, A&A, 385, 632
Martin, C., Bouret, J.-C., Deleuil, M., Simon, T., & Catala, C. 2004, A&A, 416, L5
Mayer, L., Quinn, T., Wadsley, J., & Stadel, J. 2004, ApJ, 609, 1045
Meeus, G., Waters, L. B. F. M., Bouwman, J., et al. 2001, A&A, 365, 476
Najita, J., Carr, J. S., & Tokunaga, A. T. 1996, ApJ, 456, 292
Najita, J. R., Edwards, S., Basri, G., & Carr, J. 2000, Protostars and Planets IV, 457
Najita, J., Carr, J. S., & Mathieu, R. D. 2003, ApJ, 589, 931
Pollack, J. B., Hubickyj, O., Bodenheimer, P., et al. 1996, Icarus, 124, 62
Qi, C., et al. 2004, ApJ, 616, L7
Rettig, T. W., Haywood, J., Simon, T., Brittain, S. D., & Gibb, E. 2004, ApJ, 616, L163
Richter, M. J., Jaffe, D. T., Blake, G. A., & Lacy, J. H. 2002, ApJ, 572, L161
Thi, W. F., Van Dishoeck, E. F., Blake, G. A., et al. 2001, ApJ, 561, 1074
Thi, W.-F., van Zadelhoff, G.-J., & van Dishoeck, E. F. 2004, A&A, 425, 955
Vidal-Madjar, A., Désert, J.-M., Lecavelier des Etangs, A., et al. 2004, ApJ, 604, L69
Waters, L. B. F. M., & Waelkens, C. 1998, ARA&A, 36, 233
Willacy, K., Klahr, H. H., Millar, T. J., & Henning, T. 1998, A&A, 338, 995